IET Nanobiotechnology

Research Article

IET Journals
The Institution of Engineering and Technology

Facile synthesis of multi-walled carbon nanotube via folic acid grafted nanoparticle for precise delivery of doxorubicin

ISSN 1751-8741
Received on 10th December 2018
Revised 4th April 2019
Accepted on 30th April 2019
E-First on 29th July 2019
doi: 10.1049/iet-nbt.2018.5421
www.ietdl.org

Pravin S. Uttekar[1], Sameer H. Lakade[2] ✉, Vijay K. Beldar[1], Minal T. Harde[3]

[1]Department of Pharmaceutics, PES's Modern College of Pharmacy, Sector No. 21, Yamuna Nagar, Nigdi, Pune, (M.S), India
[2]Department of Pharmaceutics, RMD Institute of Pharmaceutical Education & Research, Pune, (M.S), India
[3]Department of Pharmaceutical Chemistry, PES's Modern College of Pharmacy, Sector No. 21, Yamuna Nagar, Nigdi, Pune, (M.S), India
✉ *E-mail: sameer_patil97@rediffmail.com*

Abstract: The motive of work was to develop a multi-walled carbon nanoplatform through facile method for transportation of potential anticancer drug doxorubicin (DOX). Folic acid (FA)-ethylene diamine (EDA) anchored and acid functionalised MWCNTs were covalently grafted with DOX via π–π stacking interaction. The resultant composite was corroborated by ^{1}H NMR, FTIR, XRD, EDX, SEM, and DSC study. The drug entrapment efficiency of FA-conjugated MWCNT was found high and stability study revealed its suitability in biological system. FA-EDA-MWCNTs-DOX conjugate demonstrated a significant *in vitro* anticancer activity on human breast cancer MCF-7 cells. MTT study revealed the lesser cytotoxicity of folate-conjugated MWCNTs. The obtained results demonstrated the targeting specificity of FA-conjugate via overexpressed folate receptor deemed greater scientific value to overcome multidrug protection during cancer therapy. The proposed strategy is a gentle contribution towards development of biocompatible targeted drug delivery and offers potential to address the current challenges in cancer therapy.

1 Introduction

Development of innovative drug carriers for targeted cancer therapy with high competent and particularity is of paramount significant and has been one of the leading arguments in current nanomedicine. Since few decades, carbon nanotube (CNTs) becomes a reliable tool for targeted nano-drug delivery in the field of cancer therapy and achieved potential space and popularity in biomedical and pharmaceutical applications [1–3]. It possesses an outstanding thermal, mechanical, electrical property and emerges as a promising agent for targeting the drug at specific site [4, 5]. Due to the intrinsic physical property and stability of CNTs, it provides extended residence time in human body with more architectural flexibility [6, 7]. Due to enhanced drug accumulating quality and ability to cross the cell membrane, it effectively enhances the therapeutic efficacy of the drug [8]. Recent study shows certain limitations of pristine CNTs can possibly be resolved through surface functionalisation by chemical modifications such as adsorption, amidation, acylation, esterification, carboxylation, PEGylation and polymer coatings on CNTs, leads to enhance its physicochemical property in various solvent and also improves their polymer dispersion quantitatively in polymer matrics [9, 10]. Due to great capacity of targeting the drug at required site, CNTs has attracted great interest in biomedical and healthcare applications [11].

In our present investigation, stable and biocompatible functionalised MWCNTs were developed, covalently conjugated with folic acid (FA) to assess anticancer potential of doxorubicin (DOX). Modification of MWCNTs was sequentially carried out with FA and EDA. The synthesised FA-EDA-MWCNTs-DOX conjugate was characterised using different analytical techniques. The entrapment efficiency and drug release were monitored through UV-Vis spectroscopy. The release behaviour of nanoconjugate was studied at pH 5.3 and 7.4. At the end, biocompatibility and targeted therapeutic efficiency of FA-EDA-MWCNTs-DOX conjugate was assessed using MTT assay on MCF-7 cell lines. Therefore, present selective approach provides newer avenue for efficient anticancer potential of synthesised nanoconjugate, which exhibited greater MTT and also address current therapies in tumour targeting.

2 Materials and methods

2.1 Materials

Multi-walled CNTs (MWCNTs) (purity > 95.0 wt.%, length = 5–15 µm, diameter = 10–20 nm) were obtained from USB, USA. DOX hydrochloride purity 99.56% was received as benevolent gift from Emcure Pharmaceuticals Pvt. Ltd., Pune, India. FA, N-hydroxy succinamide (NHS), N, N'-di cyclohexyl carbodiimide (DCC), 1-Ethyl-3-(3-Dimethyl aminopropyl) carbodiimide (EDAC), 2-(N-Morfolino) Ethane sulfonic acid (MES) were acquired from Sisco research Lab. Pvt. Ltd., Mumbai,3-(4,5-dimethylthiazole-2-yl)-2,5 diphenyl tetrazolium bromide (MTT), Dulbecco's Modified Eagle Medium (DMEM), Foetal Bovine Serum (FBS) were procured from Sigma Aldrich Pvt. Ltd., Mumbai. Regenerated cellulose dialysis membrane (12 kDa MWCO) was acquired from Spectrum Laboratories Inc., Rancho Dominguez, CA, U.S.A. MCF-7 (Breast cancer cell lines) was procured from NCCS (National Centre for Cell Science) Pune, India. All other chemicals and solvents adapted for the experiments were of analytical grades.

3 Method

3.1 Conjugation of FA-EDA-MWCNTs-DOX

In order to remove amorphous impurities, unpurified MWCNTs were treated in a microwave at 400 ± 2°C for 2 h. 500 mg of microwave-activated MWCNTs was refluxed in a round-bottom flask (equipped with reflux condenser and thermometer) with 200 mL mixture of concentrated nitric and sulphuric acid (HNO_3: H_2SO_4, 1:3 ratio) with continuous stirring (100 rpm; Remi, Mumbai, India) at 120 ± 5°C for 24 h. The solution was concentrated using ultra centrifuge (20,000 rpm for 15 min). The obtained product was washed five to ten times with deionised water in order to approach pH equal to neutrality. Finally, the obtained product was lyophilised and stored [12]. 44 mg of FA was dissolved in a mixture of dimethyl sulphoxide (40 ml) and triethylamine (0.5 ml). Further, N-hydroxy succinamide (520 mg) was added with continuous stirring at 100 rpm; (Remi, Mumbai, India) for 18 h until all unreacted dicyclohexylurea (DCU) was removed by dialysis tube (MWCO 5–6 K_{DI}) using deionised water.

© The Institution of Engineering and Technology 2019

The obtained solid product was vacuum-dried and stored [13]. The FA-NHS (150 mg) conjugate was synthesised by covalently cross-linking FA-NHS using 1, 2 ethylene diamine (EDA 75 ml) and tri-ethyl amine (0.5 ml) co-dissolved into DMSO (5 mL) under vigorous magnetic stirring at 100 rpm for 24 h. The unreacted EDA was separated by dialysis tube (MWCO 5–6 K_{DI}) against deionised water. The obtained product was poured into excess of ether to produce pale yellow precipitate and dried under vacuum. The resultant product was diluted appropriately and detected using UV-Vis spectrophotometer (Jasco V 630) at λ max 363 nm [14]. A solution of oxidised MWCNTs (20 mg) was prepared with 50 mg of N-ethyl-N′-(3-dimethyl-aminopropyl) carbodiimide hydrochloride (EDAC) in 20 mL anhydrous DMSO with continuous stirring (100 rpm) at 50°C for 10 h. Further FA-EDA-NH_2 (4.60 mg/mL) was added and continuously stirred at 100 rpm (Remi, Mumbai, India) for 5 days. The unreacted FA-EDA-NH_2 was removed by dialysis tube (MWCO 5–6 K_{DI}) against deionised water. The obtained nanoconjugate was vacuum-dried and characterised using FT-IR [15]. Briefly F-MWCNTs (functionalised-MWCNTs) dispersed in MES buffer solution pH 6.1 (50 mM 2 mg/mL, 90 mL) then mixture was transferred into 500 mM MES buffer solution of DOX (2.5 mg/mL, 10 mL) at room temperature. Followed by 9.2 mL of NHS (50 mg/ml) aqueous solution and 4.8 mL (10 mg/ml) of EDAC solution was added to preformed mixture under magnetic condition. Further suspension was concentrated by using rotary evaporator. The obtained mixture was centrifuged at 25,000 rpm at room temperature for 15 min and washed multiple times with 50 mM MES buffer solution (pH 6.1) until the solution becomes transparent. The amount of unbound DOX was determined by UV-Vis spectroscopy [16].

4 Characterisation of DOX (FA-EDA-MWCNTs-DOX) conjugate

The FT-IR instrument (Jasco 4100, Tokyo, Japan) was used to obtain FT-IR spectra of FA-EDA-MWCNTs-DOX conjugates between the scanning range 4000–400 cm^{-1}. The maximum absorbance of synthesised conjugates was acquired using UV-Vis. spectrophotometer (Jasco V 630, Toyo, Japan) between 200 and 800 nm as a qualitative analysis of FA-conjugate. The ^1H NMR spectra was recorded using ARX-400 spectrometer. Dimethylsulphoxide (DMSO-d6) was used as solvent to determine proton at 300 MHz. The powder X-ray diffraction analysis (Philips PW 3710, Almdo, Netherland) was conducted for phase analysis study. Differential scanning calorimetry (DSC 821e Mettler Toledo, Switzerland) was used to record the thermal changes in sample. The particle size, zeta potential, and polydispersity index (PDI) were analysed (Horiba Scientific Nano partica SZ 100) at an angle 30° between 100 and 300 kcps. The entrapment efficiency was determined by centrifugation (Eppendrof 5810 R, Hamburg, Germany) at 1500 rpm for 1 h at 4°C and quantisation study was performed at wavelength 490 nm. The accelerated stability study was conducted at 5 ± 2°C, 25 ± 2°C, and 40 ± 2°C for a period of 8 weeks in stability chamber (Remi CHM-6S, India).

4.1 In vitro diffusion study

The *in vitro* release study of DOX from FA-EDA conjugated MWCNTs were check out by using the dialysis bag diffusion technique (12 kDa MWCO) hermetically sealed suspended in PBS (2 mL 40 mM, pH 7.4) and acetate buffer (2 mL 40 mM, pH 5.3). The entire experimental temperature was kept at 37 ± 0.5°C with continuous magnetic stirring at 100 rpm/min. At selected time interval (2, 4, 6, 8, 10, 24, 48, 72 and 96 h), the drug sample (1 ml outer phase) was removed from receptor compartment with replacement of same medium. The concentration of released DOX was quantified by using UV-Vis absorption spectroscopy at λ max 331 nm [17].

4.2 Cell culture experiment

The *in vitro* anticancer activity of DOX conjugated MWCNTs was investigated against human breast cancer MCF 7 cells using MTT assay. The cells were grown in RPMI 1640 medium supported with 10% v/v FBS and 2 mM l-glutamic acid. The cells were inoculated at density 1×10^5 cells/mL per well plates using in situ binding agent trichloro acetic acid (TCA) and incubated for 24 hr at 37°C, 5% CO_2. The each preoccupied wells were replaced with fresh medium (100 µL) containing various concentration (1–10 µg/ml) of DOX. Before that drug was solubilised in dimethyl sulphoxide (maintaining concentration below 0.2%). For comparison growth media without drug was used as a control. Further cell plates were kept in incubator for 48 h to allow the attachment of cells to the well surface. The assay was terminated by cold TCA (50 µL) and incubated for 2 h at 4°C. Thereafter, medium containing sample was removed and washed with sterile 100 µL of PBS and dried. After that medium containing MTT (4,5-dimethyl/ thiazollyl-2 yl) −2,5-diphenyltetra zoliumbromide in PBS maintaining pH 7.4 was added to each well and incubated for 1 h. Subsequently, formazan dye was removed and DMSO (100 µL) was added to dissolve retained formazan crystals. The final read against blank with scanning spectroscopy (Elisa plate reader) at wavelength of 540 nm with 690 nm reference. The plate by plate method was used to calculate percentage growth of test results and calculated as [18]:

$$\begin{aligned}&\text{Cellgrowth}(\%)\\&\quad=\tfrac{1}{4}(\text{Avg.absorbanceofthetestwell/}\\&\quad\text{Avg.absorbanceofthecontrolwells})\\&\quad\times 100.\end{aligned}$$

5 Results and discussion

5.1 Fourier transform infra-red (FT-IR)

The surface functionalisation of nanoconjugate to nanocarrier was proved by FT-IR spectroscopy study. The results evidently establish that the treatment of MWCNTs with blended acid introduces the carboxyl groups on the nanotube surface besides cutting down the MWCNTs. The FTIR spectra of FA exhibit characteristic peaks at 3643.12, 3326.24, 3230.78, 2926.37, 1965.34, 1693.27, 1683.23, 1641.21, 1414.27, 1293.24, and 1162.33 cm^{-1}. These bands are typical FA characteristics and accordant with report [19]. The peaks between the range 3600 and 3000 cm^{-1} are hydroxyl(-OH) stretch, NH stretch, and C-H stretching vibrations. The peak appeared at 1693.27 and 1965.34 cm^{-1} assigned to C=O stretching vibration of carboxyl group, whereas peak at 1641.21 cm^{-1} ascribed to C=O stretching vibration of -CO-NH_2. The peak at 1483.23 cm^{-1} is assigned to characteristics absorption peak of phenyl ring. The peak at 1414.27 cm^{-1} corresponds to OH deformation band of phenyl skeleton. The raw form of CNTs has ability to functionalise with oxygen containing groups at external surface and ends of CNTs where the defects are introduced. The FT-IR spectrum of pure CNTs represents characteristic peaks at 3427.6 and 3197.4 cm^{-1} were attributed to (OH) hydroxyl group of characteristics peaks between 3427.6 and 3197.4 cm^{-1} and are attributed to (OH) hydroxyl group adhere on extraneous surface of pure MWCNTs. The peak at 2960 and 2890 cm^{-1} is typical of C-H stretch vibration, which was assigned to asymmetric and symmetric stretching. The peak at 1648 cm^{-1} corresponds to the characteristics of carbon residue on surface of CNTs. The unmodified MWCNTs showed absorption peak at 1456.03, 1341.25, and 1226.5 cm^{-1} confirming the presence of residue on the surface. Oxidised MWCNTs exhibit characteristic peak at 3447 and 2934 cm^{-1} and correspond to O-H and C-H stretch. The peak at 1707.66 cm^{-1} corresponds to C=O stretch vibration of carboxyl group. Figs. 1*d* and *e* showed peaks at 1677.77, 1618.95, 1468.53, and 1465.03. These bands are exemplary characteristics of FA. FA-EDA-MWCNTs conjugate shows decrease in intensity of peak

© The Institution of Engineering and Technology 2019

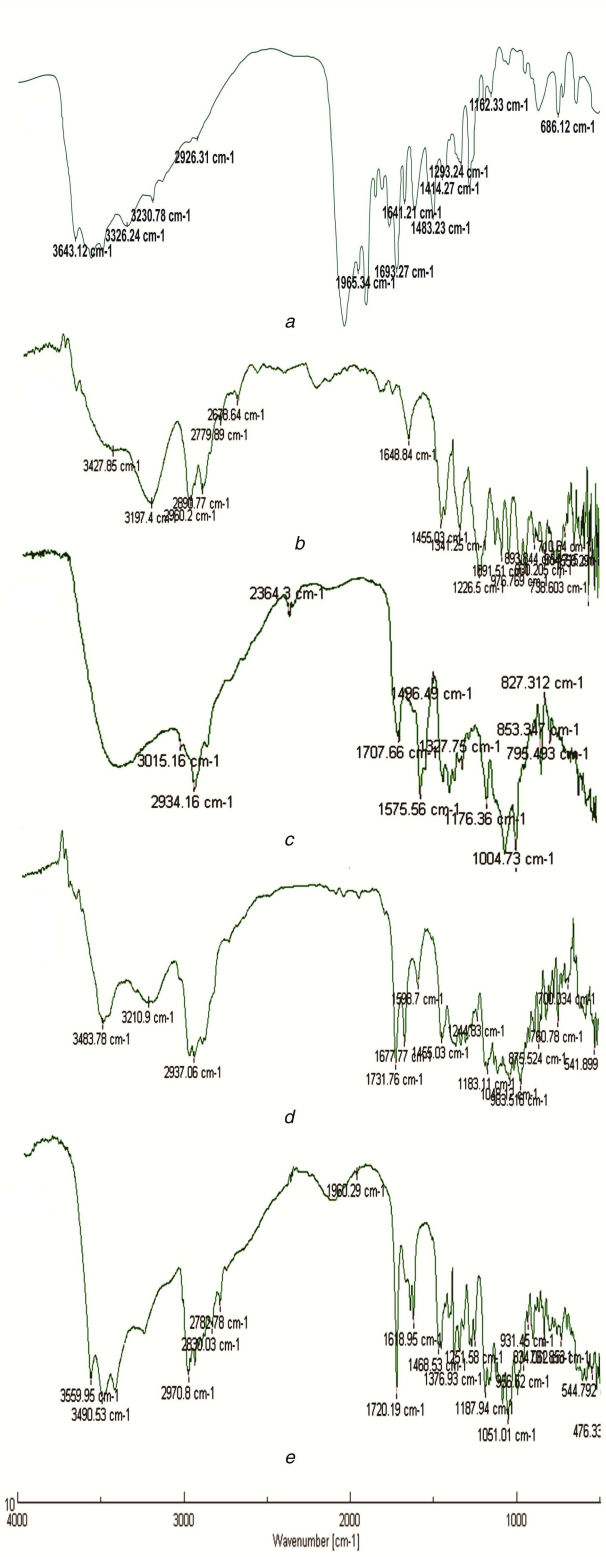

Fig. 1 *FT-IR spectra of*
(a) Folic acid, ***(b)*** Pure MWCNTs, ***(c)*** Oxidised MWCNTs, ***(d)*** FA-EDA-MWCNTs conjugate, ***(e)*** FA-EDA-MWCNTs-DOX conjugate

from 1707 to 1677 cm^{-1} due to amide carbonyl (C=O) stretch. Further, the functionalisation of oxidised MWCNTs with ethylenediamine is accepted with the presence of a new band at a lower frequency (1667 cm^{-1}) corresponding to the stretching of the amide carbonyl group (N-C=O) and the absence of band at 1707 cm^{-1} assigned to C=O in the COOH groups. Peak at 1598 and 1183 cm^{-1} designated to (N-H) in plane and (C-N) stretch proved the amino-terminal group as consistent with report [20]. Peak at 1048 and 1455 cm^{-1} being assigned to O-H deformation and C-O stretching corresponds to the attachment of FA-EDA to MWCNTs. As the functionalisation proceeds FA-EDA-MWCNTs-DOX conjugate showed prominent peaks at 3559, 3490 cm^{-1}, and at 2970 cm^{-1} correspondence to O-H stretching, N-H stretching, and C-H stretching of conjugate, respectively. The peak at 1720 cm^{-1} showed the C=O stretch of amide linkage i.e. CO-NH bond formation. The represented values of FT-IR indicate successful linkage of DOX to nano-carrier.

5.2 UV-Visible spectroscopy

Preliminary assessment of FA-EDA-MWCNTs-DOX conjugate was acquired using the overlaid UV-visible spectra in which FA-conjugate shows absorbance from 250 to 800 nm (at 280 nm, Fig. 2*b*) as obtained results are similar to report [21]. UV-visible spectrophotometer was engaged to authenticate the conjugation of FA onto the exterior of MWCNTs. From Fig. 2, it can be noticed that the characteristic absorption peak of FA due to $\pi \rightarrow \pi^*$ transition of its pterin ring is emerged at 280–283 nm. However, a slight shift could be perceived in FA-EDA-MWCNTs-DOX correlated to that of pure FA, which demonstrates the modification in environment of the FA between the free and grafted states [22]. These results recommend that FA ligands have been strongly grafted onto the surface of MWCNTs-. Further, FTIR spectroscopic studies are also backing these results (Fig. 1). DOX shows the characteristics absorbance peak at 490 nm (Fig. 2*a*). The UV spectrum of FA-EDA-MWCNTs-DOX conjugate shows the appearance of peak at 490 nm indicates the successful coupling of DOX to FA conjugate (Fig. 2*C*). The unbound DOX shows slight absorbance at 490 nm which indicates the major percentage of DOX has successfully conjugated to nano-carrier.

5.3 Nuclear magnetic resonance (NMR) spectroscopy

The appearance of characteristics proton signals in ^{1}H NMR spectrum of FA-EDA-MWCNTs-DOX conjugate confirms successful incorporation of DOX with FA-EDA-MWCNTs.

As shown in ^{1}H NMR spectrum (Fig. 3*a*) of oxidised MWCNTs, typical signal obtained at 12.07 ppm confirmed the presence of carboxylic proton. The chemical shift between 9.70 and 9.29 ppm exhibits aromatic (–CH) of oxidised-MWCNTs. The oxidised MWCNTs that do not display any other salient features related to proton signals were consistent with previous reports [23]. FA-EDA conjugate (Fig. 3*b*) exhibits characteristics signal at 9.70 and 9.29 ppm, 9.89 and 8.88 ppm, 7.59, 6.88, and 6.49 ppm, reveals the presence of aromatic protons, pteridine ring proton of FA, aromatic and amine proton of FA and -CONH proton, respectively, and indicates successful conjugation of FA and EDA. The ^{1}H NMR spectrum (Fig. 3*c*) represents FA-EDA-MWCNT conjugate, characteristics signals at 12.08, 11.06, 9.94, 8.63, 6.00, 4.98, 7.68, 6.98 and 6.67 ppm and explains FA-EDA conjugate, as current findings are in line with report [24]. The FA-EDA conjugation to MWCNTs shifts CONH proton peak at 7.18 ppm. The signal obtained at 8.99 ppm represents coupling of MWCNTs to FA-EDA conjugate. The NMR spectrum of FA exhibits typical peaks at 1.40 and 1.90 ppm. The peaks at 2.50, 2.60 and 3.30 ppm should be neglected as they are corresponding to DMSO and H_2O peaks, as reported, respectively [25]. In Fig. 3*d*, along with FA-EDA-MWCNTs peaks, the additional appearance of characteristics signal at 7.44 ppm indicates successful linkage of DOX to FA-EDA-MWCNTs complex.

5.4 Scanning electron microscopy (SEM)

The surface morphology of engineered MWCNTs was studied using SEM analysis. The SEM image of pure MWCNTs and FA-EDA-MWCNTs-DOX conjugate shown in Figs. 4*a*, *b* and *c*, *d,* respectively, indicates the change in morphology between SEM image of pure MWCNTs and FA-EDA-MWCNTs-DOX conjugate. The structure after conjugation showed clear contrast between the SEM image of pure MWCNTs and FA-EDA-MWCNTs-DOX. The SEM image of pure MWCNTs showed CNTs was tubular in shape with open ends and nanometre size range. The experimental (after

© The Institution of Engineering and Technology 2019

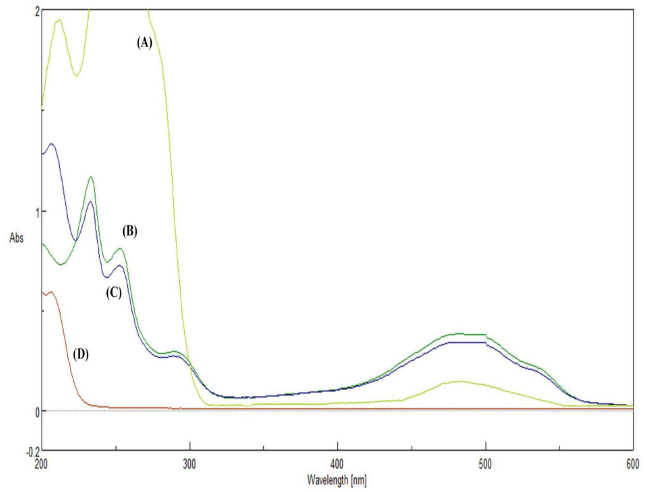

Fig. 2 *UV/visible spectrum of*
(a) Doxorubicin, ***(b)*** FA-EDA-MWCNTs conjugate, ***(c)*** FA-EDA-MWCNTs-DOX conjugate, ***(d)*** Unbound doxorubicin

functionalisation) results showed an exfoliated and curled surface morphology. It is also bundled together and tubes are less isolated with distinct nature as compared to the pristine nanotubes, which were noticeable in SEM image of FA-EDA-MWCNTs-DOX. It is noticeable that tubular structure of nanotubes was intact even after functionalisation. We found that as functionalised nanotubes are bundled together due to heightening interlinkage among the tubes as reported [26]. All morphological changes represent the major differences that were observed in structural integrity of CNTs and FA-EDA-MWCNTs-DOX conjugate. After conjugation process, we observed that DOX tethered onto the surface of MWCNTs almost towering density. This may be quality arrangement of MWCNTs during synthesis of FA-EDA-MWCNTs-DOX. The white spots are clearly the results of agglomeration of F-MWCNT in FA-EDA-MWCNT-DOX. Whereas agglomeration of MWCNT advocates that part of surface area of CNT could not be accessed during functionalisation; this is due to inherent Van der Waals forces keeping the MWCNTs jointly as bundle. Based on this outcome suggested bettered interaction between FA-EDA-MWCNTs-DOX as reported in [27].

This results in further confirmation of successful surface functionalisation.

5.5 Energy dispersive X-ray spectroscopy (E.D.X)

To determine the elemental concentration of synthesised nano-carrier, EDX analysis was carried out. The EDX spectrum of pure MWCNTs shows the presence of 96.70% carbon and 3.04% low oxygen content. The carboxylated carbonaceous fragments were conjugated with outer surface of oxidised MWCNTs. Several etching of surface and disordered sites may result due to interaction of strong oxidising agent with MWCNTs. The EDX spectrum of FA-EDA-MWCNTs-DOX conjugate revealed the presence of 90.72% carbon and 5.05% oxygen contents in relation to pure MWCNTs. The small amount of nitrogen 3.20%, sulphide 0.15%, ca-wollastonite 0.06% was evidenced for formation of new functional groups. Above outlined result indicates the small quantities of oxygenated groups, which expanded when they were treated with a sulfo-nitric admixture. When ox-MWCNTs were functionalised with ethylenediamine, an expansion in the percentage of nitrogen and oxygen was noticed, which demonstrate that the incorporation of the EDA chain to the sample was successful. These results were also in consistent with the report [28]. The existence of a appreciable amount of N in the sample can be another indication for the construction of FA-EDA-MWCNTs. Elemental analysis of FA-EDA-MWCNTs-DOX conjugate shows the presence of nitrogen atom on the surface of nanotube depending on amide structure (see, Fig. 5). Functionalised MWCNTs coupled with nitrogen content of DOX provides estimated amount of attached amides. The exhilarating, the greater

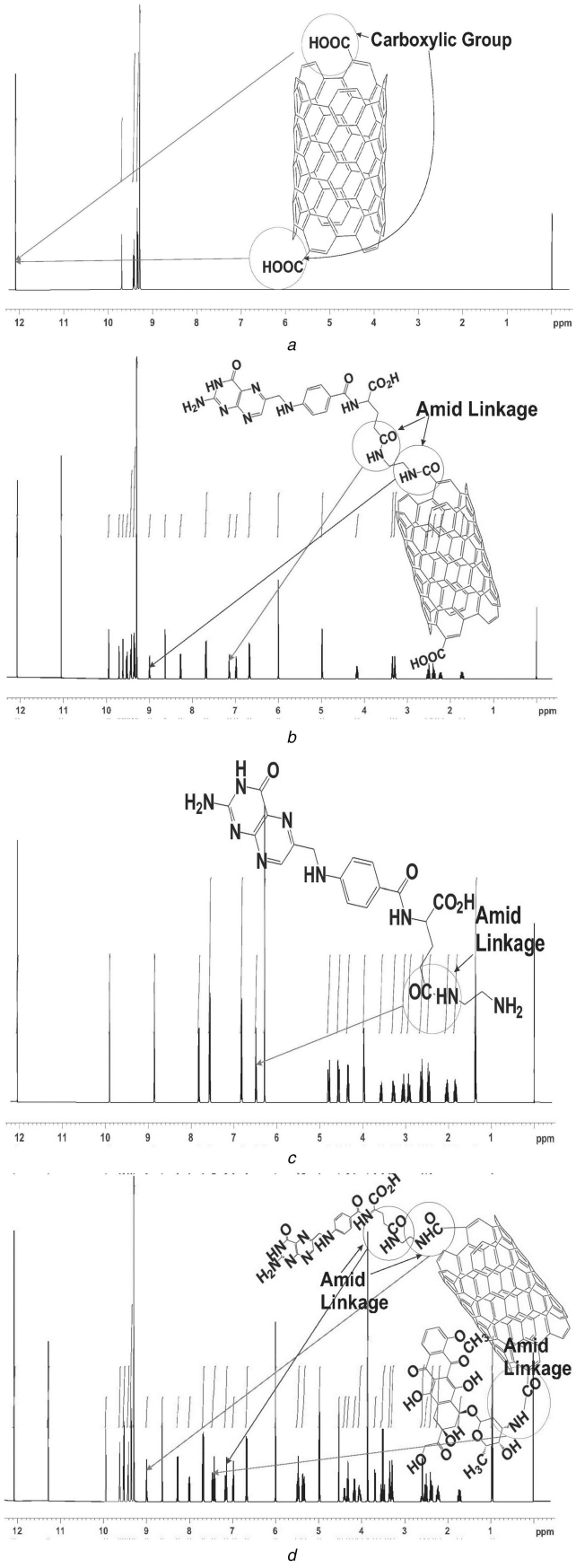

Fig. 3 *^{1}H NMR spectra of*
(a) Oxidised MWCNTs, ***(b)*** FA-EDA conjugate, ***(c)*** FA-EDA-MWCNTs conjugate, ***(d)*** FA-EDA-MWCNTs-DOX conjugate

amount of oxygen, and sulphur content are detected in sample. This advocates that the content of acidic groups (-COOH) basic groups (-OH and C=O) increased with increasing oxidation time

© The Institution of Engineering and Technology 2019

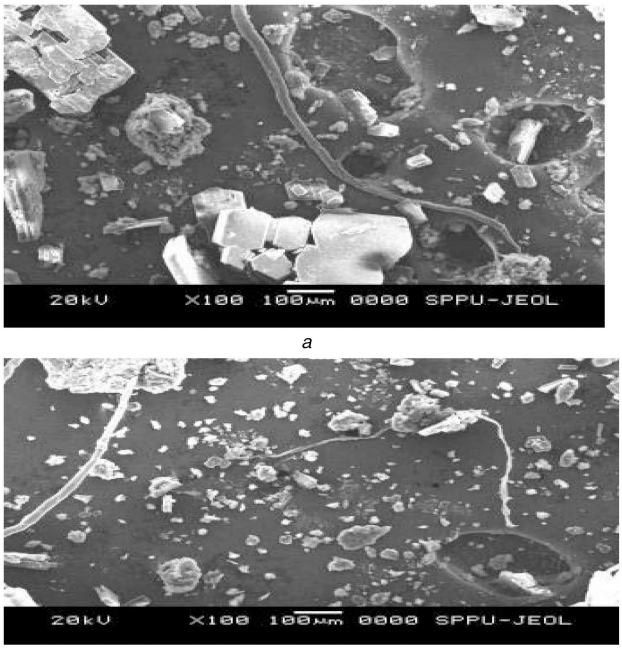

Fig. 4 *SEM images of*
(a) Pure MWCNTs and ***(b)*** FA-EDA-MWCNTs-DOX conjugate

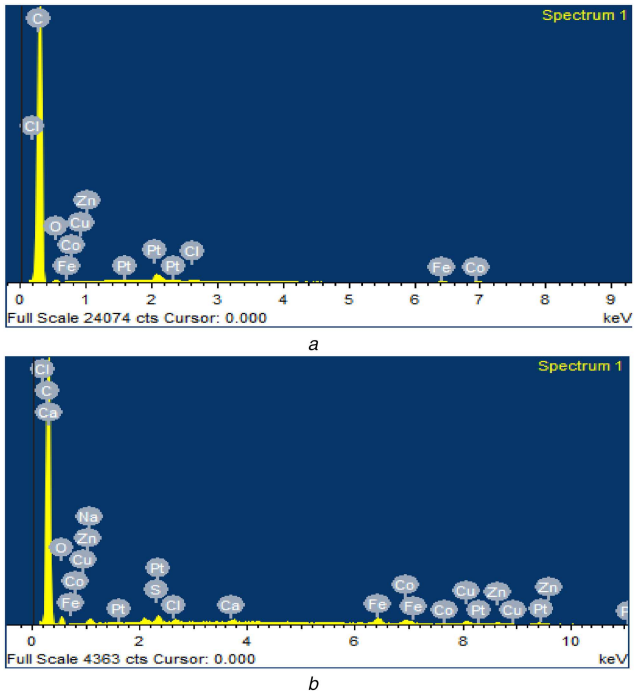

Fig. 5 *EDX spectrum of*
(a) Pure MWCNTs and ***(b)*** FA-EDA-MWCNTs-DOX conjugate

and process [29]. The elemental analysis results confirm well conjugation of drug molecule with MWCNTs at surface level.

5.6 P. X.R.D. spectroscopy

The X-ray diffraction study (Fig. 6) was carried out to determine the nature of pure DOX and FA-EDA-MWCNTs-DOX conjugate. The diffractogram of DOX depicted highly sharp intensity peak at 2θ angle 34.9°, 23.7°, 17.7°, 15.1°, 28.3°, 16.1°, 14.9°, 18.3° (represented in Fig. 6*a*) and suggest crystalline nature. The diffraction pattern of FA-EDA-MWCNTs-DOX conjugate (Fig. 6*b*) exhibited broad peak at 2θ angle 22.7°, 21.9°, 15.2°, 16.2°, 23.1°, 18.6°, 19.7°, 24.2°, 29.3° and less intense diffused intensity peak indicates the presence of amorphous form which implies that the drug was dispersed at a molecular level in the MWCNTs surface.

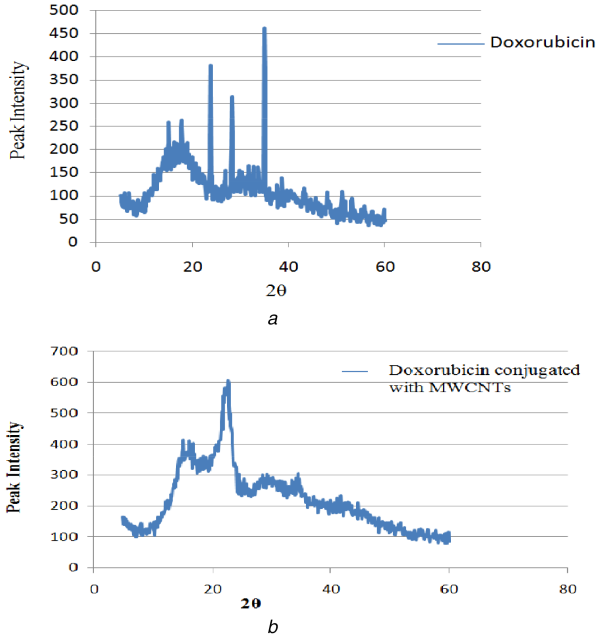

Fig. 6 *XRD spectra of*
(a) Pure doxorubicin and ***(b)*** FA-EDA-MWCNTs-DOX conjugate

XRD pattern of MWNTs-COOH revealed the presence of dual peaks at 25.7 and 43.6°, corresponding to the interiorlayer spacing (0.34 nm) of the MWNTs (d002) and the d100 reflection of the MWNTs. However due to FA-EDA-functionalisation, the disappearance of observed both peak confirmed the surface functionalisation of nanoconjugate. However, the XRD pattern of the nanoconjugate exhibited the similar to those observed from the pure MWCNTs, demonstrating that no supplementary crystalline order or chain arrangement had been introduced into the FA-EDA-MWCNTs-DOX conjugate. This result declared that there was a DOX coated on the superficial of MWCNTs, respectively, in good agreement with the literature [30]. According to Bragg's law, the resulted less intense peaks of nanoconjugate may be due to conjugation process which increases the basal spacing.

5.7 Differential scanning calorimetry (DSC)

The DSC thermogram of pure DOX and FA-EDA-MWCNTs-DOX authenticates (Figs. 7*a* and *b,* respectively) the presence of drug carrier interaction. A sharp endothermic peak at 228–230°C for pure DOX (Fig. 7*a*) corresponds to the reported melting point (226–232°C). The FA-EDA-MWCNTs-DOX conjugate (Fig. 7*b*) represents two endothermic peaks. The first endothermic peak at 222–224°C indicates the melting point of DOX, which bound covalently to the surface of FA-EDA-MWCNTs that bring greater stability as correlated to pure DOX. Second endotherm at 264–266°C attributed to the melting point of present conjugate. Observed evidence declined all possibility of interaction (i.e. chemical incompatibility) between the drug and developed FA-EDA-MWCNTs-DOX nanoconjugate. A decline in overall crystallinity may be as an outcome of two factors: DOX agglomerates acting as effective nucleation sites and at the equivalent time, the non-agglomerated sites inhibiting flexibility of nanoconjugate. As the well-dispersed FA-EDA-DOX MWCNTs crystal growth was constrained, thus leading to a decline of crystallinity. The observed results are in accordant with report [31]. Further, XRD studies are also backing these results (Fig. 6)

5.8 Particle size and polydispersity index (PDI) analysis

The particle size analysis of pure DOX, before and after the functionalisation, was carried out to probe the changes on MWCNTs surface. The particle size of unreacted DOX (Fig. 8*a*) before carboxylation and conjugation was found to be 262 nm. The surface functionalised particle size of FA-EDA-MWCNTs-DOX conjugate (Fig. 8*b*) showed increase in particle size to 391 nm. The

© The Institution of Engineering and Technology 2019

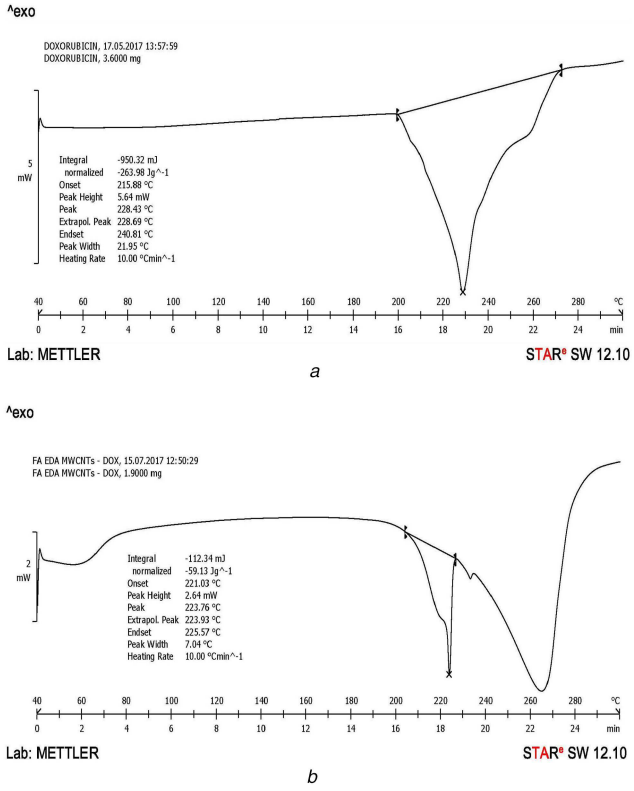

Fig. 7 *DSC graph of*
(a) Pure doxorubicin and ***(b)*** FA-EDA-MWCNTs-DOX conjugate

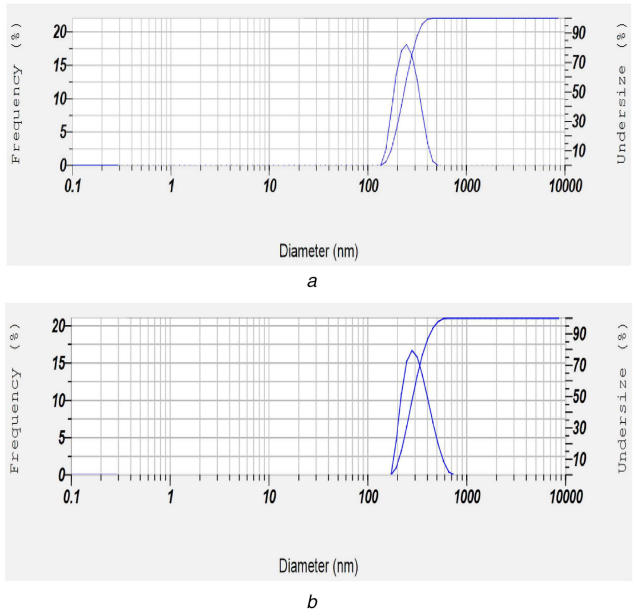

Fig. 8 *Particle size results of*
(a) Pure MWCNTs and ***(b)*** FA-EDA-MWCNTs-DOX conjugate

increase in particle size of nanoconjugate confirmed the drug encapsulation over the surface of pure MWCNTs. It was further adopted from the entrapment efficiency result that the greater amount of drug 83.44% entrapped significantly leads to enlarge particle size confirmed the well conjugation. It was expressed that MWCNT size is consistent in the length of 200 m and 500 nm which are advisable for drug delivery in cancer therapeutics [32].

PDI was used to determine the distribution of individual molecular masses in conjugates. PDI value of pure MWCNTs was found as 0.409 and FA-EDA-MWCNTs-DOX conjugate was found as 0.427. PDI of both pure and conjugate was found to be lesser than 0.5 particles, which further proved to be significant (p<0.05). The PDI study revealed that the particles were found to be of mild range monodisperse and hence was well accepted.

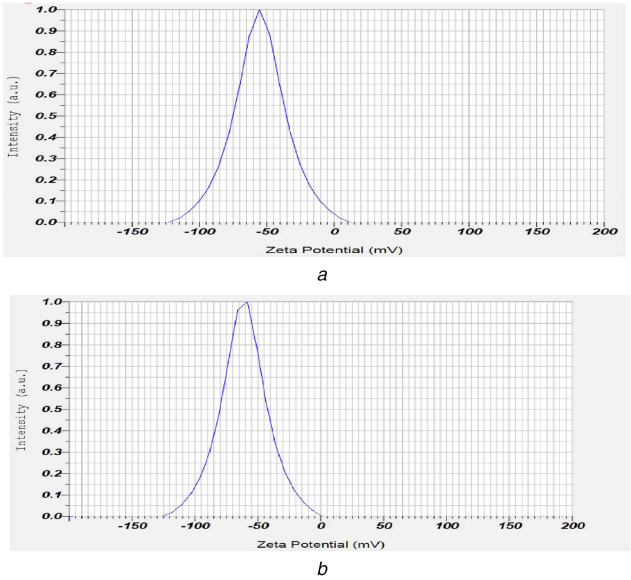

Fig. 9 *Zeta potential results of*
(a) Oxidised MWCNTs and ***(b)*** FA-EDA-MWCNTs-DOX conjugate

5.9 Zeta potential

Zeta-potential analysis was carried out to identify the surface charge on MWCNTs after chemical alterations. The oxidised-MWCNTs depicted the slightly negative zeta potential −55.3 mV (Fig. 9*a*), which could be due to ionisation reaction of carboxylic acids in water (especially with respect to 4 <pKa< 5). The zeta potential value of FA-EDA-MWCNTs-DOX nanoconjugate was −61.3 mV (Fig. 9*b*), a value higher than that of oxidised MWCNTs. It has been postulated that the negative zeta potential of FA-EDA-MWCNTs-DOX possibly be due to the negative inductive effect and availability of ionisable group on DOX in non-protonated state. This can also be associated, in part, to the expanded hydrocarbon chain of FA-MWCNT. This significant change in zeta potential values reflects the successful conjugation of DOX molecule on FA decorated MWCNTs. Greater zeta-potential emerge in refined stability of nanoparticles and narrower size distribution, hypothetically because the charged particles repelled one another and, therefore, overpower the legitimate tendency to aggregate. Zeta potential can extremely influence particle stability through electrostatic repulsion between particles as reported [33].

5.10 In vitro diffusion study

The gigantic percentage drug encapsulation ability of MWCNTs demonstrates potential application of CNTs as a drug carrier. The *in vitro* release behaviour of DOX from the surface functionalised MWCNTs conjugate exhibited bi-phasic pattern that was characterised by an initial faster followed by slow drug release. The release profile of DOX from the nano-conjugates was explored under two different pH conditions (pH = 5.3 and 7.4), which represent the acidic environment and physiological environment, respectively. The release of DOX from FA-EDA-MWCNTs-DOX nano-conjugate showed pH-dependent behaviour. The *in vitro* diffusion study revealed that the faster release kinetics may be due to free FA-EDA conjugation on surface of MWCNTs, which increases DOX release at pH 5.3 than at pH 7.4. As shown in Fig. 10 after 48 h at pH 5.3, about 68.12% drug was released, whereas there was only 11.42% release of drug from FA-EDA-MWCNTs-DOX attributed to the formation of -CONH amide bond by nucleophilic substitution reaction between DOX and F-MWCNTs. Further -CONH bond dissociate easily at pH 5.3 than pH 7.4, which correspond to difference in the release obtained. The above outlined result of drug release contributes for treating tumour at acidic condition (pH 5.3). Slow release recommends insignificant exposure of loaded drug to exterior microenvironment that could be due to superlative steric hindrance on ends and side walls resulting low and sustained release. The DOX discharge data

© The Institution of Engineering and Technology 2019

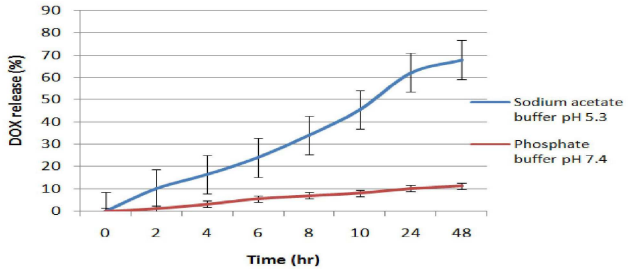

Fig. 10 *Cumulative DOX release (%) from FA-EDA-MWCNTs-DOX nanoconjugates at 37 ± 0.5°C in sodium acetate buffer pH 5.3 and phosphate buffer pH 7.4*

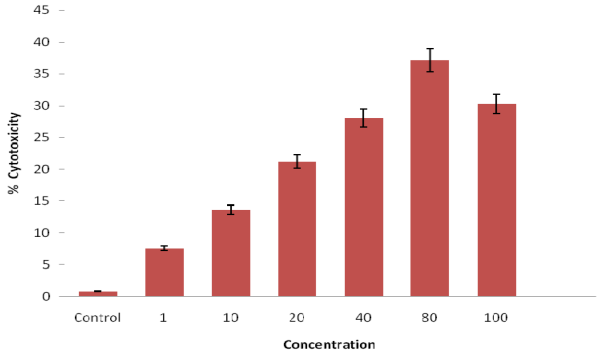

Fig. 11 *% Cell cytotoxicity of FA-EDA-MWCNTs-DOX nanoconjugates on MCF- cell lines by MTT assay*

best suits into Higuchian release kinetics. The current release data are in line with previous reports [34]. The *in vitro* release performance of FA-EDA-MWCNTs-DOX will no doubt be useful in tumour targeting where the micro-environments are dormant acidic and possibly facilitate greater drug release from newly developed nanoconjugate. Furthermore, the comparably moderate DOX release at pH 5.8 may be associated to the evidence that a small portion of DOX is covalently linked with the trigger carboxyl groups of FA.

5.11 Drug entrapment efficiency

The percentage drug entrapment within functionalised MWCNTs was studied by measuring non-entrapped DOX in recovered supernatant after centrifugation by UV-Vis spectrophotometer at 490 nm. The percentage drug entrapment was found to be 83.44%. DOX due to its aromatic nature interact strongly with outer surface and ends of nanotubes significantly improved the drug entrapment efficiency through various interactions (such as nucleophilic substitution reaction, hydrogen bonding, π-π stacking and strong hydrophobic interactions among MWCNTs-DOX). The significant drug entrapment efficiency of surface functionalised CNT makes it better drug carrier for tumour targeting and possesses improved stability at physiological pH with enhanced drug release at acidic pH. Whereas endohedral enmesh into the innermost cavity of nanotubes structure leading to superior entangle is also expected; however, assessment technique is not explored yet. The detected data could conceivably be ascribed to loading of cationic DOX in and around FA-EDA-based micro-domains also via p–p stacking. Recently 91% DOX loading efficiency was reported approximately in functionalised CNTs [35].

5.12 Methyl thiazole tetrazolium (MTT) assay

Unquestionably apoptosis in most conserved form of cell death is a major response to DOX in human cell lines (MCF-7) at doses used in this study. This response of DOX may fractionally be accountable for their efficacy in treating breast cancer which is normally resistant to apoptosis (see, Fig. 11).

In the present study, the percentage cell viability and cell cytotoxicity of FA-EDA-MWCNTs-DOX conjugate was assessed at different micro-molar concentrations against MCF-7 (human breast cancer) cells using MTT assay. MWCNTs degree of functionalisation has its own rate for cytotoxic responses in culture. MTT assay clearly revealed that upon increasing the concentration from 1 to 100 µg/mL FA-EDA-MWCNTs-DOX, the relative percentage cell viability of cancerous cells were decreased over a period of 24 hr incubation, possibly due to apoptosis by intercalating DOX with DNA. Due to endocytosis mechanism and uptake by cancerous cells, increased in cytotoxic response was observed, corresponding to dose-dependent cytotoxic response. In MCF-7 cells, the drug conjugate FA-EDA-MWCNTs-DOX showed the cytotoxicity 7.58 and 30.31% at 1 µg/mL and 100 µg/mL, respectively (Figs. 9 and 10). For drug conjugate with MCF-7 cells reduced apoptosis was observed which may be due to overexpressed anti-apoptotic factor Bcl-2 (B Cell Lymphoma-2) and caspase-3 the major component of effector phase. On MCF-7 cells drug conjugate demonstrated reduced toxicity possibly due to apoptotic pathway was not well expressed. At the same time, another explanation in case of MTT assay results revealed that maximum cytotoxicity was observed at 80 µg/mL on MCF-7 cell lines (Figs. 9 and 10) was 37.13%. This may be due to facilitated uptake of nanoconjugates at these concentrations, which resulted in availability of more drug molecules inside the cell, hence leading to enhanced effect of cytotoxicity. From the result, it was demonstrated that for the measurement of cytotoxicity, cellular uptake cannot, however, be the only factor. The interaction between MWCNTs cell membrane could also alter cellular response and cytotoxicity. Further it may be due to assembled MWCNTs at this concentration which could hurt the cell membrane response to cell death. These explain the rationale for enhanced cytotoxicity of newly synthesised nanoconjugate at 80 µg/mL than 100 µg/mL. Therefore, the cytotoxicity of the synthesised MWCNTs at concentration of 80 µg/mL ascribed to the intracellular release from FA-EDA-MWCNTs-DOX which results higher uptake by cells wherein directly permits to the nucleus of tumour cells. The obtained results are in line with the reported data [36]. In addition the outcome displayed that the zeta potential of conjugate FA-EDA-MWCNTs-DOX did not showed symbolic change during the time of examination. Such consideration can provide confirmation on good dispersibility of FA-EDA MWNTs. All these results point towards the fact that MWCNTs functionalised nanotubes did not show compelling destructive effects on the viability of MCF-7 cell line. This firmly suggests that the FA-EDA MWCNTs could be availed as drug carrier.

© The Institution of Engineering and Technology 2019

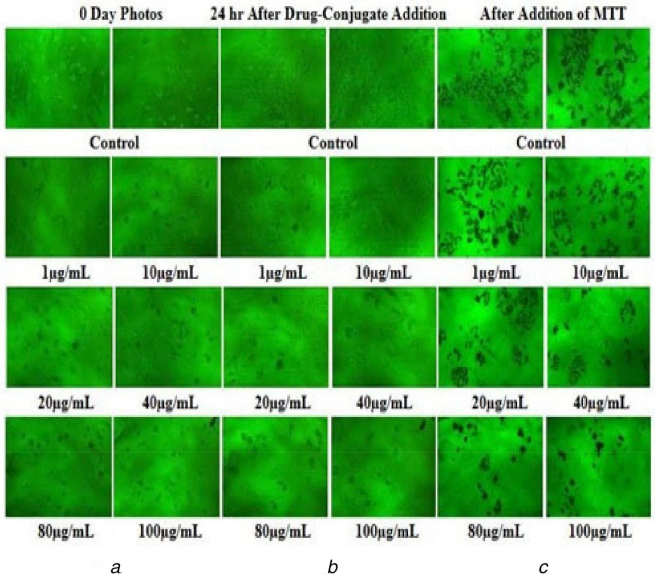

Fig. 12 *Inverted microscopic images of*
(a) MCF-7 cells at 0 days, ***(b)*** MCF-7 cells treated with FA-EDA-MWCNTs-DOX conjugate after 24 h, ***(c)*** MCF-7 cells treated with after addition of MTT

Table 1 Accelerated stability study data of FA-EDA MWCNTs-DOX nanoconjugate

Stability parameter	FA-EDA-MWCNTs-DOX					
	Conjugate after 8 weeks					
	Dark (°C)			Light (°C)		
	5 ± 2	25 ± 2	40 ± 2	5 ± 2	25 ± 2	40 ± 2
turbidity	−	−	++	−	++	++
precipitation	−	−	+	−	+	++
change in colour	−	+	+	−	+	++
crystallisation	−	−	+	−	+	+
change in consistency	−	+	++	−	+	++

5.13 In vitro anticancer study

The in vitro anticancer activity of DOX, oxidised MWCNTs, FA-EDA-MWCNTs conjugate and FA-EDA-MWCNTs-DOX conjugate were explored against folate overexpressed human breast cancer MCF-7 cells adopting in vitro MTT assay (Fig. 12). The advantages of the FA-EDA nanoconjugate formulation of DOX were quantified by the GI50 value, which is described as the drug concentration desired to inhibit 50% of the incubated cells growth in a designed time period. From Fig. 12, it is observed that the GI50 for DOX is 13.5 ± 1.4 µg/ml, while it was greatly decreased to 8.8 ± 0.71 µg/ml, for the oxidised MWCNTs. Furthermore, the GI50 value for FA-EDA-MWCNTs was 4.8 ± 0.5 µg/ml, while GI50 value of FA-EDA-MWCNTs-DOX was greatly decreased to 3.4 ± 0.53 µg/ml. The enhanced anticancer activity of FA-EDA-MWCNTs is attributed to the enhanced dispersability of DOX onto the surface of MWCNT, increased stability of DOX inside the nanoconjugate core, high drug transportation by passive targeting to cancer cells, the controlled drug release properties [37]. Further, improved anticancer activity of FA-EDA-MWCNTs-DOX demonstrated active targeting effects to the cancer cells, which may suggest that the FA-conjugated nanoconjugate were endocytosed via a folate receptor-mediated mechanism [38]. The order of cytotoxicity, as determined from the assay, was FA-EDA-MWCNTs-DOX>FA-EDA-MWCNTs> oxidised MWCNTs> DOX

5.14 Stability testing

A stability of FA-EDA-MWCNTs-DOX nano-conjugate was studied at different temperature conditions (5 ± 2°C, 25 ± 2°C and 40 ± 2°C). At temperature condition 5 ± 2°C, a stable nanoconjugate was obtained. The stability study revealed that the nanoconjugate is unstable at increased temperature. At 25 ± 2°C, the nanoconjugate showed slight turbidity; whereas, at 40 ± 2°C, increase in turbidity level with bundling and aggregation of nanotubes was observed. Due to nucleophilic substitution interaction, F-MWCNTs showed themselves most stable in all suitable environmental condition for biological applications. From the result of analysis, it was observed that the (FA-EDA-MWCNTs-DOX) nanoconjugates were more stable in dark at 5 ± 2°C than 25 ± 2°C and 40 ± 2°C temperature [39] (see Table 1). From the stability data, it was concluded that the formed nanoconjugate confirmed most stable due π-π stacking suitably be stored in coloured and air-tight vessel in cool condition.

6 Conclusion

We have successfully designed and synthesised the FA-EDA-MWCNTs-DOX nanoconjugate for high performance and characteristics of targeted release. The resulting nanoconjugate displayed pH-dependent DOX release with no signals of drug cluster formation. DOX has been effectively loaded to FA-EDA-MWCNTs via nucleophilic substitution and π-π stacking interaction. The synthesised nanocarrier can convincingly enlarge the build-up of DOX in cancer cells and leads to noticeable anticancer response over expressed on MCF-7 cell lines. At the end, our results demonstrated that FA-EDA-MWCNTs-DOX nanoconjugate served as potential and promising carrier for breast cancer treatment.

7 Acknowledgments

The author sincerely acknowledges the PES's modern college of pharmacy and Savitribai Phule Pune University Pune for providing infrastructural facilities. The author sincerely acknowledges Emcure pharmaceutical, Pune for providing the gift sample of doxorubicin hydrochloride.

© The Institution of Engineering and Technology 2019

8 References

[1] Ali, Z., Seyed, A., Ali, Z., *et al.*: 'Comparative study on non-covalent functionalization of carbon nanotubes by chitosan and its derivatives for delivery of doxorubicin', *Chem. Phys. Lett.*, 2015, **642**, pp. 22–28

[2] Ebbesen, T.W., Lezec, J., Hiura, H., *et al.*: 'Electrical conductivity of individual carbon nanotubes', *Nature*, 1996, **382**, (6586), pp. 54–56

[3] Mehra, K., Mishra, V., Jain, K.: 'A review of ligand tethered surface engineered carbon nanotubes', *Biomaterials*, 2014, **35**, pp. 1267–1283

[4] Aad, G., Abbott, B., Abdallah, J., *et al.*: 'The ATLAS simulation infrastructure', *Euro. Phys. J. C*, 2010, **70**, pp. 823–874

[5] Iijima, S.: 'Carbon nanotubes: past present, and future', *Physica B Condens. Matter*, 2002, **323**, pp. 1–5

[6] Vogelson, T.: 'Advances in drug delivery systems', *Nano Mod. Drug Disco.*, 2001, **4**, (52), pp. 49–50

[7] Thess, A., Lee, R., Nikolaev, P., *et al.*: 'Crystalline ropes of metallic carbon nanotubes', *Science*, 1996, **273**, (5274), pp. 483–487

[8] Park, C., Ounaies, Z., Watson, A., *et al.*: 'Dispersion of single wall carbon nanotubes by in situ polymerization under sonication', *Chem. Phys. Lett.*, 2002, **364**, pp. 303–308

[9] Mehra, N., Jain, N.: 'Development. Characterization and cancer targeting potential of surface engineered carbon nanotubes', *J. Drug Target.*, 2013, **21**, (8), pp. 745–758

[10] Lacerda, L., Russier, J., Pastorin, G., *et al.*: 'Translocation mechanisms of chemically functionalized carbon nanotubes across plasma membranes', *Biomaterials*, 2012, **33**, pp. 3334–3343

[11] Erttmann, R., Erb, N., Steinhoff, A.: 'Pharmacokinetics of doxorubicin in man: dose and schedule dependence', *J. Cancer Res. Clin. Oncol.*, 1988, **114**, (5), pp. 509–513

[12] Gupta, U., Dwivedi, S.K.D., Bid, H.K., *et al.*: 'Ligand anchored dendrimers based nanoconstructs for effective targeting to cancer cells', *Int. J. Pharm.*, 2010, **393**, pp. 185–196

[13] Jain, A.K., Dubey, V., Mehra, N.K.: 'Carbohydrate conjugated multi walled carbon nanotubes: development and characterization', *Nanomed., Nanotech. Biol. Med.*, 2009, **5**, pp. 432–442

[14] Sudimack, J., Lee, R.J.: 'Targeted drug delivery via the folate receptor', *Adv. Drug Deliv. Rev.*, 2000, **41**, pp. 147–162

[15] Datsyuk, V., Kalyva, M., Papagelis, K., *et al.*: 'Chemical oxidation of multi walled carbon nanotubes', *Carbon.*, 2008, **46**, pp. 833–840

[16] Shi, X., Wang, S.H., Shen, M., *et al.*: 'Multifunctional dendrimer modified multiwalled carbon nanotubes: synthesis, characterization and in vitro cancer cell targeting and imaging', *Biomacromolecules*, 2009, **10**, pp. 1744–1750

[17] Muthu, M.S., Kutty, R.V., Luo, Z.J., *et al.*: 'Theranostic vitamin E TPGS micelles of transferrin conjugation for targeted co-delivery of docetaxel and ultra bright gold nanoclusters', *Biomaterials*, 2015, **39**, pp. 234–248

[18] Jeyamohan, P., Hasumura, T., Nagaoka, Y., *et al.*: 'Accelerated killing of cancer cells using a multifunctional single-walled carbon nanotubebased system for targeted drug delivery in combination with photothermal therapy', *Int. J. Nanomed.*, 2013, **8**, pp. 2653–2667

[19] Yang, S.J., Lin, F.H., Tsai, K.C., *et al.*: ' folic acid-conjugated chitosan nanoparticles enhanced protoporphyrin IX accumulation in colorectal cancer cells', *Bioconjug. Chem.*, 2010, **21**, (4), pp. 679–689

[20] Yang, D.Q., Rochette, J.F., Sacher, E.: 'Functionalization of multiwalled carbonnanotubes by mild aqueous sonication', *J. Phys. Chem. B*, 2005, **109**, pp. 7788–7794

[21] Butt, A.M., Mohd Amin, M.C., Katas, H.: 'Synergistic effect of pH-responsive folate-functionalized poloxamer 407-TPGS-mixed micelles on targeted delivery of anticancer drugs', *Int. J. Nanomed.*, 2015, **10**, pp. 1321–1334

[22] Zhang, J., Misra, R.D.: 'Magnetic drug-targeting carrier encapsulated with thermosensitive smart polymer: core-shell nanoparticle carrier and drug release response', *Acta Biomater.*, 2007, **3**, (6), pp. 838–850

[23] Cao, X., Tao, L., Wen, S., *et al.*: 'Hyaluronic acid-modified multiwalled carbon nanotubes for targeted delivery of doxorubicin into cancer cells', *Carbohydr. Res.*, 2014, **405**, pp. 1–34

[24] Dube, D., Francis, M., Leroux, J.C., *et al.*: 'Preparation and tumor cell uptake of poly(N-isopropylacrylamide) folate conjugates', *Bioconjug. Chem.*, 2002, **13**, pp. 685–692

[25] Lin, J.J., Chen, J.S., Huang, S.J., *et al.*: 'Folic acid-pluronic F127 magnetic nanoparticle clusters for combined targeting, diagnosis, and therapy applications', *Biomaterials*, 2009, **30**, (5), pp. 114–5124

[26] Singh, D.K., Iyer, P.K., Giri, P.K.: 'Functionalization of carbon nanotubes and study of its optical and structural properties', *J. Nanotech. Appl.*, 2008, **4**, (1), pp. 55–58

[27] Ramontja, J., Ray, S., Pillai, S.K., *et al.*: 'The effect of surface functionalized carbon nanotubes on the morphology as well as thermal, thermo mechanical, and crystallization properties of polylactide'. Available at https://researchspace.csir.co.za/dspace/bitstream/handle/10204/5535/Ramontja_2011.pdf?sequence=1&isAllowed=y

[28] Montesa, I.E., Muñoz, A.M., Benito, W.K., *et al.*: 'FTIR Thermo-gravimetric analysis of biotin-functionalized single walled carbon nanotubes', *J. Nanosci. Nanotechnol.*, 2007, **7**, pp. 3473–3476

[29] Pistone, A., Ferlazzo, A., Lanza, M., *et al.*: 'Morphological modification of MWCNT functionalized with HNO_3/ H_2SO_4 mixtures', *J. Nanosci. Nanotechnol.*, 2012, **12**, pp. 5054–5060

[30] Van der Lee, M.K., Van Dillen, A.J., Bitter, J.H., *et al.*: 'Deposition precipitation for the preparation of carbon nanofiber supported nickel catalysts', *J. Am. Chem. Soc.*, 2005, **127**, pp. 13573–13582

[31] Ramontja, J., Ray, S., Pillai, S.K., *et al.*: 'The effect of surface functionalized carbon nanotubes on the morphology, as well as thermal, thermomechanical, and crystallization properties of polylactide'. Available at https://researchspace.csir.co.za/dspace/bitstream/handle/10204/5535/Ramontja_2011.pdf?sequence=1&isAllowed=y

[32] Singh, R.P., Sharma, G., Sonali, S., *et al.*: 'Vitamin E TPGS conjugated carbon nanotubes improved efficacy of docetaxel with safety for lung cancer treatment', *Colloids Surf. B Biointerfaces*, 2016, **141**, pp. 429–442

[33] Gu, Y.J., Cheng, J., Jin, J., *et al.*: 'Development and evaluation of pHresponsive single-walled carbon nanotube-doxorubicin complexes in cancer cells', *Int. J. Nanomed.*, 2011, **6**, pp. 2889–2898

[34] Huang, H., Yuan, Q., Shah, J.S., *et al.*: 'A new family of folate decorated and carbon nanotube-mediated drug delivery system: synthesis and drug delivery response', *Adv. Drug Deliv. Rev.*, 2011, **63**, pp. 1332–1339

[35] Arora, S., Kumar, R., Kaur, H., *et al.*: 'Translocation and toxicity of docetaxel multi-walled carbon nanotube conjugates in mammalian breast cancer cells', *J. Biomed. Nanotechnol.*, 2014, **10**, pp. 1–9

[36] Pindiprolu, S.K.S.S., Krishnamurthy, P.T., Chintamaneni, P.K., *et al.*: 'Nanocarrier based approaches for targeting breast cancer stem cells', *Artif. Cells Nanomed. Biotechnol.*, 2018, **46**, (5), pp. 885–898

[37] Harei, A., Osouli, M., Bayat, F., *et al.*: 'Nanomedicine approaches for sirolimus delivery: a review of pharmaceutical properties and preclinical studies', *Artif. Cells Nanomed. Biotechnol.*, 2018, **46**, (supp. 1), pp. 1–14

[38] Lodhi, N., Mehra, N.K., Jain, N.K., *et al.*: 'Development and characterization of dexamethasone mesylate anchored on multi walled carbon nanotubes', *J. Drug Target.*, 2013, **21**, pp. 67–76

[39] Yang, S.J., Lin, F.H., Tsai, K.C., *et al.*: 'Folic acidconjugated chitosan nanoparticles enhanced protoporphyrin IX accumulation in colorectal cancer cells', *Bioconjugate Chem.*, 2010, **21**, pp. 679–689

© The Institution of Engineering and Technology 2019